Design and Performance of Sampled Data Loops for Subcarrier and Carrier Tracking

S. Aguirre and W. J. Hurd
Communications Systems Research Section

Design parameters and resulting performance are presented for the sampled data analogies of continuous-time phase-locked loops of second and third order containing perfect integrators. Expressions for noise-equivalent bandwidth and steady-state errors are given. Then, stability and gain margin are investigated using z-plane root loci. Finally, an application is presented for Voyager subcarrier and carrier tracking under the dynamics of the encounters with Uranus and Neptune. For carrier tracking, loop bandwidths narrow enough for satisfactory loop SNR_s can be achieved using third-order loops without rate aiding, whereas second-order loops would require aiding. For subcarrier tracking, third-order loops can be used when the sampling rate is limited to approximately once per second, as in the Baseband Assembly, whereas second-order loops sufficiently wide to track the dynamics have stability problems at that sampling rate.

I. Introduction

Phase-locked loops for communications systems synchronization must satisfy requirements for noise performance, dynamic tracking, process or oscillator noise tracking, stability and gain margin, acquisition, and signal-to-noise ratio threshold. Digital technology enables the use of sampled data loops with programmable or even adaptively controlled parameters. These loops have significant advantages over continuous-time analog loops, but also have some characteristics requiring different design considerations.

Two major advantages of sampled data loops that enhance the dynamic tracking ability for a fixed-loop bandwidth are that perfect integrators can be realized, resulting in type-two second-order loops and type-three third-order loops when desired, and that third-order loops become more feasible because the parameters can be accurately controlled and varied with time. A major potential disadvantage of sampled data loops is that they are never unconditionally stable: high loop gains always result in instability due to the inherent transport lag. This is as opposed to first- and second-order continuous-time loops, which are normally unconditionally stable.

Stability problems with sampled data loops occur when the loop bandwidth is not sufficiently small compared to the sampling rate, i.e., the loop filter update rate. This case is of significant interest because the sampling rates for typical implementations are limited by mechanization considerations. This article investigates the stability and gain margin of second- and third-order loops when the loop bandwidth compared with sampling rate is wide enough that continuous loop

analysis is inadequate. Achievable loop bandwidths and steady-state phase-lag errors due to dynamics are discussed.

The Voyager II encounters with Uranus in January, 1986, and with Neptune in August, 1989, are of particular interest. The performance is presented for various loops for both subcarrier and carrier tracking under the dynamics at the encounters. It is shown that third-order loops result in excellent performance at both encounters, whereas second-order loops are marginal at Uranus and unsatisfactory at Neptune, for both carrier and subcarrier tracking.

II. Approach

The design of sampled data loops is more complex than that of continuous loops because the physical parameters of the loops cannot be calculated directly, as in the case of continuous loops, from the desired loop bandwidth, damping ratio, and, for third-order loops, the third-order gain parameter. Furthermore, stability must be investigated, because sampled data loops can be only conditionally stable. On the other hand, there is some simplification because perfect integrators can be used. This also enhances dynamic performance.

There is a folklore rule of thumb (Ref. 1) that sampled data loops perform much like the continuous-time equivalents whenever the loop bandwidth is less than one-tenth of the sampling rate. It is shown here that this is a good folklore regarding loop bandwidth, but not loop stability. For a nominal bandwidth of one-tenth of the sampling rate and for typical damping and transport lag, sampled data loops become unstable when the loop gain increases by only approximately 7 dB. This is true for both second- and third-order loops. The third-order loops also are unstable at low gain. Thus, stability should always be investigated for sampled data loops.

The approach taken here is to choose a nominal loop bandwidth as a fraction of sampling rate, and to pick other parameters based upon continuous time theory. Stability and gain margin are then investigated using z-plane root loci. Actual loop bandwidth and steady-state phase error due to dynamics can then be calculated as a function of loop gain for gains resulting in stability.

III. Review of Continuous Time Phase-Locked Loops

In this section we present a review of results widely used by designers of continuous-time phase-locked loops. Specifically, we review the expressions obtained from linear analysis of noise equivalent bandwidth and steady-state phase errors for perfect integrator second- and third-order loops.

Then, in Section IV, we discuss how to obtain a sampled data loop that contains perfect integrators, and whose gain parameters can be conveniently expressed in terms of the continuous-loop parameters r, $B_L T$, and k. We then calculate the noise equivalent bandwidth for the digital loops and the steady-state phase errors for specified input phase dynamics.

A. Second-Order Continuous Loop

The open-loop transfer function of the loop is written as $AKF(s)$, where AK is the loop gain and $F(s)$ is the loop filter transfer function. The parameter A is due to the phase detector and the signal amplitude, and K is selected by the designer and includes the VCO gain.

The perfect integrator (type 2) second-order continuous loop has a loop filter transfer function of the form (Refs. 2 and 3)

$$F(s) = \frac{1 + \tau_2 s}{\tau_1 s} \tag{1}$$

and typically $\tau_2 \ll \tau_1$. For a given loop gain AK, the loop damping parameter r is defined as

$$r = \frac{AK\,\tau_2^2}{\tau_1} \tag{2}$$

The closed-loop transfer function $H(s)$ is given by

$$H(s) = \frac{AKF(s)}{s + AKF(s)} \tag{3}$$

and its associated one-sided loop noise bandwidth B_L (in Hz) is

$$B_L = \frac{1}{2\pi} \int_{-\infty}^{\infty} |H(j\omega)|^2 \, d\omega \cong \frac{r+1}{4\,\tau_2} \tag{4}$$

Often in practice, the values $r = 2$ or 4 are selected since they correspond to damping ratios (from standard control theory notation) of $\zeta = 0.707$ or 1 respectively (note that $r = 4\zeta^2$).

Now consider tracking the carrier or subcarrier signal from a spacecraft with dynamics. The steady-state phase error for this loop due to an assumed instantaneous doppler of the form

$$d(t) = \frac{\omega_i}{c} (\Omega_0 + \Lambda_0 t) \tag{5}$$

where

ω_i = subcarrier (carrier) frequency (rad/s)

c = speed of light (m/s)

Ω_0 = spacecraft speed (m/s) at $t = 0$ (m/s)

Λ_0 = spacecraft acceleration (m/s^2)

can be calculated via the final-value theorem, and is

$$\phi_{ss} = \lim_{s\to 0} \frac{\omega_i}{c} \cdot s\,[1 - H(s)] \left[\frac{\Omega_0}{s^2} + \frac{\Lambda_0}{s^3}\right]$$

$$= \frac{\omega_i}{c} \cdot \frac{\Lambda_0}{r} \cdot \left(\frac{r+1}{4B_L}\right)^2 \tag{6}$$

B. Third-Order Continuous Loops

The loop filter and the corresponding closed-loop transfer function of a perfect third-order loop can be represented respectively as (Refs. 2 and 4)

$$F(s) = \frac{1 + \tau_2 s}{\tau_1 s} + \frac{1}{\tau_1 \tau_3 s^2} \tag{7}$$

$$H(s) = \frac{rk + r\tau_2 s + r(\tau_2 s)^2}{rk + r\tau_2 s + r(\tau_2 s)^2 + (\tau_2 s)^3} \tag{8}$$

where, as before, $r = AK\tau_2^2/\tau_1$ and with $k = \tau_2/\tau_3$. The corresponding one-sided loop bandwidth B_L (in Hz) is

$$B_L = \frac{r}{4\tau_2}\left(\frac{r - k + 1}{r - k}\right) \tag{9}$$

notice that if $k = 0$, then our loop reduces to a perfect integrator second-order loop.

When the spacecraft experiences jerk, the Laplace transform of the phase error is

$$\Phi(s) = \frac{\omega_i}{c}\,[1 - H(s)] \left[\frac{\Omega_0}{s^2} + \frac{\Lambda_0}{s^3} + \frac{J_0}{s^4}\right]$$

and the resulting steady-state phase error is

$$\phi_{ss} = \frac{\omega_i}{c} \frac{J_0}{rk} \left[\frac{r}{4B_L}\left(\frac{r - k + 1}{r - k}\right)\right]^3 \tag{10}$$

IV. Sampled Data Loop Noise and Dynamic Responses

A general block diagram for a sampled data loop is shown in Fig. 1. We resort to the z-transform technique because of the discrete nature of the system. In this linear model, θ_n symbolizes the value of the input phase at sampling instant t_n, and $\hat{\theta}_n$ its corresponding estimate. AK represents the loop gain, including the numerically controlled oscillator (NCO) gain, $F(z)$ is an arbitrary loop filter, and $N(z)$ is characteristic of the particular implementation, which includes the modeling of the NCO, phase detector, and computational delays. The open-loop transfer function is $G(z) = AKF(z)N(z)$. A factor $D(z)$ may be added as a cascaded compensator to enhance stability.

In this article we concentrate exclusively on the $N(z)$ that arises in the proposed implementation for the DSN Advanced Receiver (Ref. 5). In this case, the sampling interval (filter update interval) is of length T. Phase estimates are averages of $\theta - \hat{\theta}$ over one interval, and there is a transport lag of T seconds from the end of the measurement time until the NCO is updated. For this important case, $N(z)$ is given by

$$N(z) = \frac{T(z+1)}{2z^2(z-1)} \tag{11}$$

The derivation of this transfer function and extension to other transport lags is found in Appendix A.

Regarding the loop filter $F(z)$, we deal with the sampled data versions of filters comprising single and double integrators as defined by Eqs. (1) and (7).

A. Second-Order DPLL

The digital equivalent of the loop filter in the perfect second-order analog PLL has a transfer function of the form $F(z) = G_1 + G_2 Tz/(z - 1)$. To establish a correspondence between the digital PLL (DPLL) and the analog PLL, let $G_1 = \tau_2/\tau_1$ and $G_2 = 1/\tau_1$ where τ_1 and τ_2 are the time constants of the filter defined by Eq. (1). Then using Eqs. (2) and (4) we can express the open-loop transfer function as

$$G(z) = \frac{\frac{r}{2}(z+1)\left[\frac{4B_L T}{r+1}(z-1) + \left(\frac{4B_L T}{r+1}\right)^2 z\right]}{(z-1)^2 z^2} \tag{12}$$

Note that B_L is the noise bandwidth of the analog loop, not the bandwidth of the digital loop. The closed-loop transfer function $H(z) = G(z)/(1 + G(z))$ can be represented as

$$H(z) = \frac{b_2 z^2 + b_3 z + b_4}{a_0 Z^4 + a_1 z^3 + a_2 z^2 + a_3 z + a_4} \qquad (13)$$

where

$$b_2 = \frac{r}{2}(d^2 + d) \qquad a_2 = 1 + \frac{r}{2} d + \frac{r}{2} d^2$$

$$b_3 = \frac{r}{2} d^2 \qquad a_3 = \frac{r}{2} d^2$$

$$b_4 = -\frac{r}{2} d \qquad a_4 = -\frac{r}{2} d$$

$$a_0 = 1 \qquad d = \frac{4B_L T}{r+1}$$

$$a_1 = -2$$

Notice that this is actually a fourth-order loop in z, but we discuss it as a second-order loop because it is analogous to a type-2 second-order continuous loop.

1. Noise Equivalent Bandwidth of the Second-Order DPLL. For the DPLL, the one-sided noise equivalent bandwidth B_L^* (Hz) is given by

$$B_L^* \triangleq \frac{1}{2T} \frac{1}{H^2(1)} \frac{1}{2\pi j} \oint_{|z|=1} H(z) H(z^{-1}) \frac{dz}{z} \qquad (14)$$

where T is the update time in seconds, and $H^2(1) = 1$, regardless of r and $B_L T$.

Define

$$I_4 \triangleq \frac{1}{2\pi j} \oint_{|z|=1} H(z) H(z^{-1}) \frac{dz}{z} \qquad (15)$$

then from Table III in Ref. 6 we have

$$I_4 = \frac{a_0 B_0 Q_0 - a_0 B_1 Q_1 + a_0 B_2 Q_2 - a_0 B_3 Q_3 + B_4 Q_4}{a_0 [(a_0^2 - a_4^2) Q_0 - (a_0 a_1 - a_3 a_4) Q_1 + (a_0 a_2 - a_2 a_4) Q_2 - (a_0 a_3 - a_1 a_4) Q_3]} \qquad (16)$$

where

$$B_0 = b_0^2 + b_1^2 + b_2^2 + b_3^2 + b_4^2$$

$$B_1 = 2(b_0 b_1 + b_1 b_2 + b_2 b_3 + b_3 b_4)$$

$$B_2 = 2(b_0 b_2 + b_1 b_3 + b_2 b_4)$$

$$B_3 = 2(b_0 b_3 + b_1 b_4)$$

$$B_4 = 2 b_0 b_4$$

$$Q_0 = a_0 e_1 e_4 - a_0 a_3 e_2 + a_4 (a_1 e_2 - e_3 e_4)$$

$$Q_1 = a_0 a_1 e_4 - a_0 a_2 a_3 + a_4 (a_1 a_2 - a_3 e_4)$$

$$Q_2 = a_0 a_1 e_2 - a_0 a_2 e_1 + a_4 (a_2 e_3 - a_3 e_2)$$

$$Q_3 = a_1 (a_1 e_2 - e_3 e_4) - a_2 (a_1 e_1 - a_3 e_3) + a_3 (e_1 e_4 - a_3 e_2)$$

$$Q_4 = -a_4 Q_0 + a_3 Q_1 - a_2 Q_2 + a_1 Q_3$$

$$e_1 = a_0 + a_2$$

$$e_2 = a_1 + a_3$$

$$e_3 = a_2 + a_4$$

$$e_4 = a_0 + a_4$$

$$e_5 = a_0 + a_2 + a_4$$

The integral I_4 can also be evaluated using the residue theorem, i.e.,

$$I_4 = \sum [\text{residues of } H(z) H(z^{-1}) z^{-1} \text{ at the poles inside the unit circle}] \qquad (17)$$

For a single pole of $H(z)H(z^{-1})z^{-1}$ at $z = a$, the residue is simply

$$\text{residue} = \lim_{z \to a} (z - a) H(z) H(z^{-1}) z^{-1}$$

while for a pole at $z = a$ of multiplicity k, the residue is

$$\text{residue} = \lim_{z \to a} \frac{1}{(k-1)!} \frac{d^{k-1}}{dz^{k-1}} \cdot \{(z - a)^k H(z) H(z^{-1}) z^{-1}\}$$

this procedure requires a numerical solution because of the order of the polynomials involved.

A comparison of B_L^* with B_L is shown in Fig. 2 where the value of the parameter k is zero for the second-order loop. The two bandwidths are very close for $B_L T < 0.1$.

2. Dynamic Response of Second-Order DPLL. Under the assumption of linearity, the phase error (no noise) in the z-domain is given by the following expression

$$\Phi(z) = [1 - H(z)]\ \Theta(z) \tag{18}$$

where $H(z)$ is the closed-loop transfer function given by Eq. (13) and $\theta(z)$ is the z-transform of the phase input. If we assume an instantaneous doppler characterized by Eq. (5), and apply the final value theorem to our phase-error equation, we get

$$\phi_{ss} = \frac{\omega_i}{c} \lim_{z \to 1} \left(\frac{z-1}{z}\right) [1 - H(z)]$$

$$\left[\frac{\Omega_0 Tz}{(z-1)^2} + \frac{\Lambda_0 T^2 z\,(z+1)}{2\,(z-1)^3}\right]$$

$$= \frac{\omega_i}{c}\ \frac{\Lambda_0 T^2}{r}\ \left(\frac{r+1}{4B_L T}\right)^2 \tag{19}$$

This is exactly the same result obtained for continuous loops, Eq. (6). Thus, sampling and $N(z)$ do not affect the steady-state response. Again, note that B_L is the bandwidth of the continuous loop.

B. Third-Order DPLL

We now consider an extension of the loop filter employed in the second-order DPLL. We add an additional perfect integrator, so that our new filter has a transfer function of the form $F(z) = G_1 + G_2 Tz/(z-1) + G_3 T^2 z^2 (z-1)^2$. As before, we let $G_1 = \tau_2/\tau_1$, $G_2 = 1/\tau_1$, and set the new constant $G_3 = 1/\tau_1\tau_3$. The closed-loop transfer function $H(z)$ in terms of the analog parameters r, k, and $B_L T$ involves the manipulation of Eq. (9) along with $r = AK\tau_2^2/\tau_1$ and $k = \tau_2/\tau_3$. We obtain

$$H(z) = \frac{b_2 z^3 + b_3 z^2 + b_4 z + b_5}{a_0 z^5 + a_1 z^4 + a_2 z^3 + a_3 z^2 + a_4 z + a_5} \tag{20}$$

where

$$b_2 = \frac{r}{2}(d + d^2 + kd^3)$$

$$b_3 = \frac{r}{2}(kd^3 - d)$$

$$b_4 = -\frac{r}{2}(d^2 + d)$$

$$b_5 = \frac{r}{2}d$$

$$a_0 = 1$$

$$a_1 = -3$$

$$a_2 = 3 + \frac{r}{2}(d + d^2 + kd^3)$$

$$a_3 = -1 + \frac{r}{2}(kd^3 - d)$$

$$a_4 = -\frac{r}{2}(d^2 + d)$$

$$a_5 = \frac{r}{2}d$$

$$d = \frac{4B_L T}{r} \cdot \frac{r-k}{r-k+1}$$

Notice too, that this is actually a fifth-order loop, but it is analogous to the third-order, type-3 continuous loop.

1. Noise Equivalent Bandwidth of the Third-Order DPLL. The one-sided noise equivalent bandwidth B_L^* (Hz) can be written as

$$B_L^* = \frac{1}{2T H^2(1)} \cdot I_5 \tag{21}$$

with I_5 defined in Eq. (15). Again, $H^2(1) = 1$ regardless of r, $B_L T$, and k. Unfortunately, no closed form solution is readily available for the evaluation of I_5. Nevertheless, from Ref. 7, I_5 can be obtained numerically, by solving the following set of simultaneous equations:

$$\sum_{i=0}^{5} (a_{i-r} + a_{i+r}) M_i = B_r$$

$$r = 0, 1, 2 \cdots 5$$

$$M_0 = a_0 I_5 \tag{22}$$

$$B_r = \begin{cases} \sum_{i=0}^{5} b_i^2, & r = 0 \\ 2 \sum_{i=0}^{5-r} b_i b_{i+r}, & r = 1, 2 \cdots 5 \end{cases}$$

where the coefficients a_i and b_i are as shown in Eq. (20). I_5 can also be evaluated using the residue theorem, as outlined at the end of Section A-1.

In Fig. 2 we summarize the numerical results obtained with Eq. (22). For convenience, we plot the normalized product $B_L^* T$ (digital) versus $B_L T$ (analog) for several cases of interest, including $k = 0$, which corresponds to the second-order DPLL. Notice that for values of $B_L T < 0.07$, the resulting $B_L^* T$ is insensitive to either r or k and the digital system resembles the analog system, with $B_L^* T \cong B_L T$. On the other hand, when $B_L T > 0.1$, the ratio of $B_L^* T$ to $B_L T$ increases rapidly with $B_L T$, suggesting that the system is approaching the instability point. This point occurs when $B_L T \cong 0.25$ for all values of r and k. These results are also confirmed later, using the root locus technique.

2. Dynamic Response of the Third-Order DPLL. The linear loop equation for the phase error in the absence of noise is given by Eq. (18), where $H(z)$ is now given in Eq. (20), and

$$\Theta(z) = \frac{\omega_i}{c}\left[\frac{\Omega_0 Tz}{(z-1)^2} + \frac{\Lambda_0 T^2 z(z+1)}{2(z-1)^3} + \frac{J_0 T^3 z(z^2+4z+1)}{6(z-1)^4}\right]$$

is the z-transform of $\omega_i/c(\Omega_0 t + 1/2\Lambda_0 t^2 + 1/6J_0 t^3)$, which assumes that a jerk is present.

Using the final value theorem, the static phase error (in radians) is

$$\phi_{ss} = \frac{\omega_i}{c} \cdot \frac{J_0 T^3}{rk}\left[\frac{r(r-k+1)}{4B_L T(r-k)}\right]^3 \text{(rad)} \tag{23}$$

This result is exactly the one obtained for a perfect third-order continuous loop (see Eq. (10)). Note that B_L is the bandwidth of the continuous loop.

V. Stability of Sampled Data Loops

A basic requirement of a control system is that it must be stable under all operating conditions. It is important for the loop to be stable not only at the design point, but at a region of parameter values around the design point as well. This assures stability for variations in the parameters. We utilize the concept of gain margin to determine the region of stability. Gain margin is the ratio of the maximum (or minimum) loop gain for stability to the design-point loop gain. We use the root locus plot to determine stability and gain margin.

The root locus is a pictorial representation of the poles of the closed-loop transfer function as a function of the loop gain. The plot starts at zero gain on the open-loop poles and terminates at infinite gain on the open-loop zeros. For a sampled data loop, the plot is drawn in the z-plane, and the stable region is the interior of the unit circle.

The approach taken here is to choose nominal values for r, $B_L T$, and k, and then to plot the root locus as a function of loop gain. We then evaluate the system gain margin. For second- and third-order loops, note that loop gain is proportional to the parameter r.

A. Stability First-Order DPLL

For a first-sampled data loop with $F(z) = 1$, and with the $N(z)$ of Eq. (11), the closed-loop transfer function is

$$H(z) = \frac{AKT(z+1)}{2z^3 - 2z^2 + AKTZ + AKT} \tag{24}$$

The root locus plot is shown in Fig. 3.

In contrast with a first-order analog loop, which is unconditionally stable, the digital loop becomes unstable for high-loop gains. By using the Routh-Hurwitz criterion, we can determine exactly the minimum value of $r(r_{osc})$ that produces instability. The result is

$$(AK)_{osc} = \frac{\sqrt{8}-2}{T} \simeq \frac{0.828}{T} \tag{25}$$

For continuous loops, we know that (Ref. 2)

$$B_L = \frac{AK}{4} \tag{26}$$

Defining gain margin (gm) as the ratio r_{osc}/r, we obtain after combining Eqs. (25) and (26)

$$gm \simeq \frac{0.21}{B_L T} \tag{27}$$

B. Stability of Second-Order DPLL

In Fig. 4 we show a typical example of the root locus plot for the second-order sampled data loop. In this example, the design point bandwidth is $(B_L T)_0 = 0.10$, and the design point r, denoted r_0, is 4. The main point of the plot is that the loop is stable at low gains and unstable at high gains. This is also true for other nomimal parameters $(B_L T)_0$ and r_0. In this example, there are two underdamped (complex) roots and two overdamped (real) roots for both small and large r, but for $2.55 \leqslant r \leqslant 2.75$, all the roots are real. For some values of $(B_L T)_0$ and r_0, there are two complex roots for all r.

For the first-order loop we found that the gain margin is inversely proportional to $B_L T$. Finding an exact expression similar to Eq. (26) using the Routh-Hurwitz criterion or Jury's test is difficult because of the order of the polynomials involved. Nevertheless, by generating a large number of root loci for different nominal values, we found that

$$gm \simeq \frac{0.25}{B_L T} \tag{28}$$

which is valid when $r = r_0$ (actual design point equal to the nominal point) and $B_L T < 0.10$. Notice that this gain margin is slightly larger than that of the first-order loop.

C. Stability of Third-Order DPLL

In Fig. 5 we present three typical examples for the third-order loop. They show that, in general, the third-order DPLL is unstable for both low and high gains. At low gains, instability occurs if $r < k$, while for high gains, instability occurs if $r \geqslant k + 0.25 r_0/(B_L T)_0$.

Thus, the "high-gain" margin of the third-order DPLL is approximately the same for the first- and second-order DPLLs. For third-order loops, one also needs to consider the "low-gain" margin, or the amount by which the gain can be reduced before instability occurs. This "low-gain" margin is approximately k/r_0. Reduction of k improves "low-gain" margin at the expense of steady-state phase errors due to jerk (Eq. (23)). This follows intuition, since $k = 0$ corresponds to a second-order loop.

D. Stability Improvement by Compensation

For critical applications, typically when $B_L T$ is not sufficiently small to have adequate gain margins, some improvement in stability may be achieved by lead, lag, or tuned compensation networks $D(z)$. Study of loops with compensation is outside the scope of this article.

VI. Application to Voyager

In this section, we determine the loop-bandwidth requirements for second- and third-order PLLs for dynamic tracking at the Voyager II encounters with Uranus and Neptune. Our criteria for good dynamic tracking is that the steady-state phase error be 1 degree or less. For DPLLs, the sampling rate should be greater than 10 B_L to have an adequate gain margin of approximately 7 dB. In this case, $B_L^* \cong B_L$, so the bandwidths are approximately the same for continuous and sampled data loops.

A. Bandwidth Requirements for Second-Order PPLs

From Eq. (19), for second-order loops the B_L required for a given steady-state phase error due to acceleration is

$$B_L = \frac{r+1}{4} \frac{1}{\sqrt{r}} \Lambda_0^{1/2} \sqrt{\frac{\omega_i}{c} \cdot \frac{1}{\phi_{ss}}} \tag{29}$$

For example, for the Voyager subcarrier frequency of 360 kHz and a steady-state error of 1°, Eq. (29) simplifies to

$$B_L = 0.164 \frac{r+1}{\sqrt{r}} \Lambda_0^{1/2}$$

In Table 1 we present the required minimum second-order loop bandwidth for Voyager subcarrier and carrier tracking (at 8.4 GHz) in order to achieve 1° steady-state phase error at the encounters. We assume acceleration values of $\Lambda_0 = 0.32$ m/s² and 4 m/s² for Uranus and Neptune, respectively.

B. Bandwidth Requirements for Third-Order PLLs

From Eq. (23), for third-order loops the B_L required for a given steady-state phase error due to jerk is

$$B_L = \frac{r}{4} \left(\frac{r-k+1}{r-k} \right) \left(\frac{\omega_i}{c} \cdot \frac{J_0}{rk\phi_{ss}} \right)^{1/3} \tag{31}$$

For 1° steady-state error when the spacecraft experiences jerk, and for the 360-kHz subcarrier frequency,

$$B_L = 0.189 \frac{r}{(rk)^{1/3}} \cdot \left(\frac{r-k+1}{r-k} \right) J_0^{1/3}$$

In Fig. 6 we plot the normalized ratio $B_L/J_0{}^{1/3}$ for different values of r and k. Notice that for fixed k the required bandwidth increases as r increases. Table 2 summarizes the bandwidth requirements for third-order loops at encounters. We

assume jerk values of $J_0 = 0.83 \times 10^{-4}$ m/s^3 and 0.29×10^{-2} m/s^3 for Uranus and Neptune, respectively.

The reader should not conclude from Fig. 6 that small values of r are optimum, considering all effects. Specifically, the problem of acquisition must be considered. This will be done in a future report.

C. Conclusions for Subcarrier Tracking

For subcarrier tracking, there appear to be no fundamental problems with either second- or third-order DPLLs. The widest bandwidth required to track at Neptune with a second-order loop is 0.82 Hz, which results in an adequate loop SNR of 39 dB under weak signal conditions of symbol SNR of 0 dB and symbol rate of 20 ksymbols/s. For the existing Baseband Assembly (BBA) Demodulator Synchronizer (DSA), the only potential problem is the sampling rate. The DSA sampling rate is currently limited to slightly over 1/s. With this sampling rate, use of third-order loops is indicated for both encounters.

D. Conclusions for Carrier Tracking

For carrier tracking, loop SNR is a serious problem, and it is important to use the narrowest loop bandwidth that is consistent with both dynamic tracking and with tracking of the oscillator instabilities.

With the current DSN receivers, the Voyager spacecraft is tracked in the cruise mode with threshold bandwidths of $B_L = 6$ Hz. The actual B_L depends on SNR, but is on the order of 10 Hz. Thus, it is known that 10-Hz bandwidths are satisfactory for tracking oscillator instabilities.

Dynamic tracking at the encounters with second-order loops require bandwidths of 30 to 130 Hz. With third-order loops, the dynamic tracking limitation is only 1 to 4 Hz. Thus, use of third-order loops is indicated. Considering both dynamics and oscillator instabilities, a bandwidth of approximately $B_L = 10$ Hz may be appropriate. The loop must be implemented with an adequate sampling rate of at least 100/s.

References

1. Lindsey, W.C., and C.M. Chie, "A Survey of Digital Phase-Locked Loops," *Proceedings of the IEEE*, Vol. 69. No. 4, pp. 410–431, April 1981.
2. Holmes, J.K., *Coherent Spread Spectrum Systems*, John Wiley & Sons Inc., New York, 1982.
3. Tausworthe, R.C., *Theory and Practical Design of Phase-Locked Receivers*, JPL Technical Report No. 32-819. Jet Propulsion Laboratory, Pasadena, Calif., Feb. 1966.
4. Tausworthe, R.C., and R.B. Crow, *Practical Design of Third-Order Phase-Locked Loops*, JPL Technical Report 900-450. Jet Propulsion Laboratory, Pasadena, Calif., April 27, 1971.
5. Sfeir, R., S. Aguirre, and W.J. Hurd, "Coherent Digital Demodulation of a Residual Carrier Signal Using IF Sampling", *TDA Progress Report 42-78*, pp. 135-142. Jet Propulsion Laboratory, Pasadena, Calif., April 1984.
6. Jury, E.I., *Theory and Application of the Z-Transform Method*, Wiley, New York, 1964.
7. Winkelstein, R.A., "Closed Form Evaluation of Symmetric Two-Sided Complex Integrals", *TDA Progress Report 42-65*, pp. 133-144. Jet Propulsion Laboratory, Pasadena, Calif., July 1981.

Table 1. Second-order PLL bandwidths for 1° steady-state phase error at encounters

r_0	Bandwidth B_L, Hz			
	Subcarrier		Carrier	
	Uranus	Neptune	Uranus	Neptune
2	0.20	0.70	30	106
4	0.23	0.82	35	126

Table 2. Third-order PLL bandwidths for 1° steady-state phase error at encounters

r_0	k	Bandwidth B_L, Hz			
		Subcarrier		Carrier	
		Uranus	Neptune	Uranus	Neptune
2	1/4	0.033	0.11	0.94	3.0
	1/3	0.030	0.10	0.86	2.8
4	1/4	0.042	0.14	1.2	3.9
	1/3	0.038	0.13	1.1	3.6

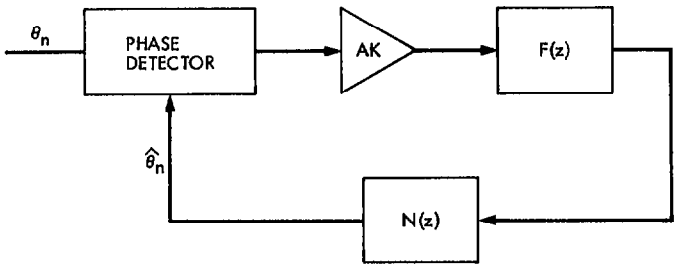

Fig. 1. Linearized model of the sampled data loop

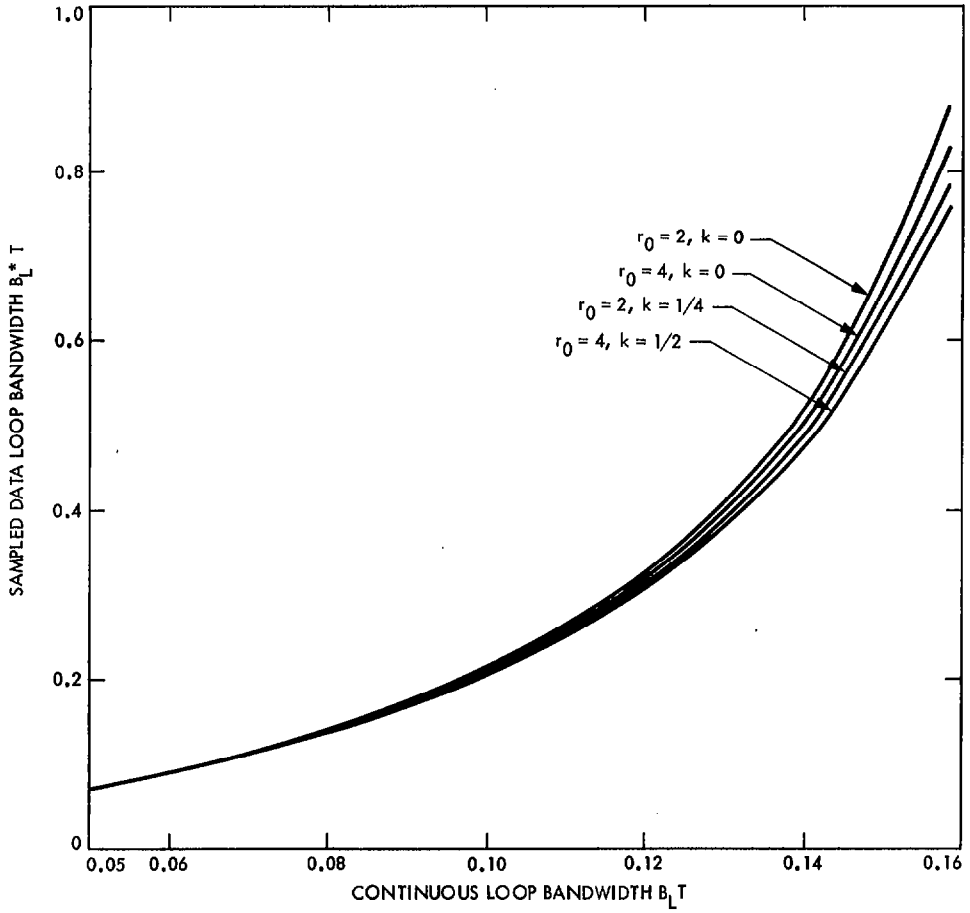

Fig. 2. Normalized bandwidth of the sampled data loop

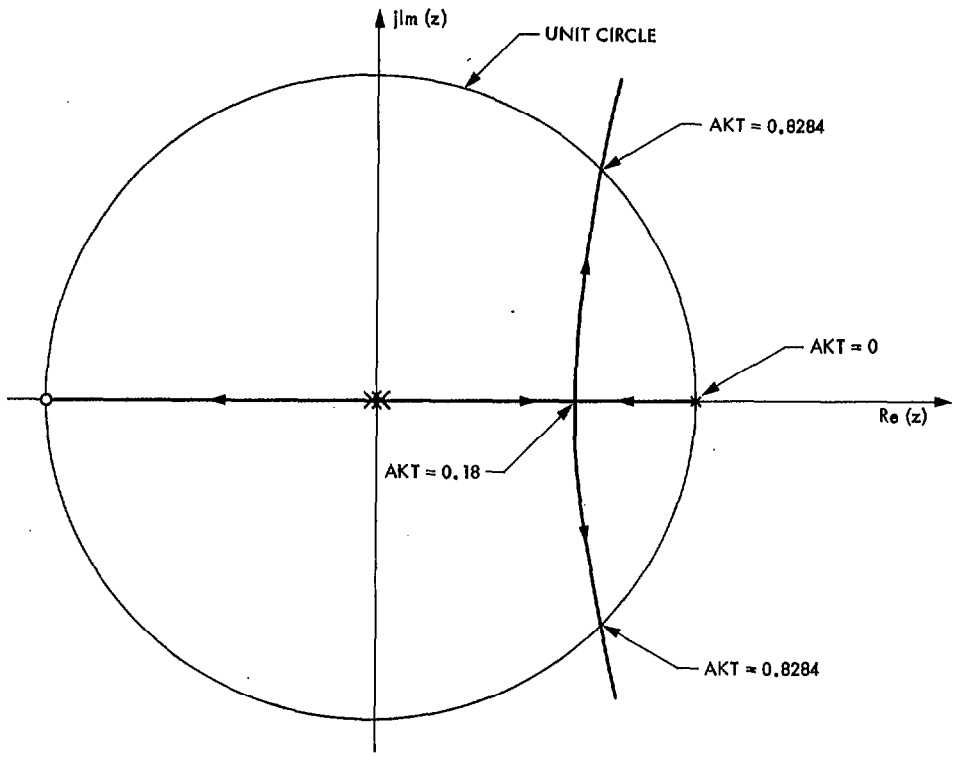

Fig. 3. Root locus of the first-order DPLL

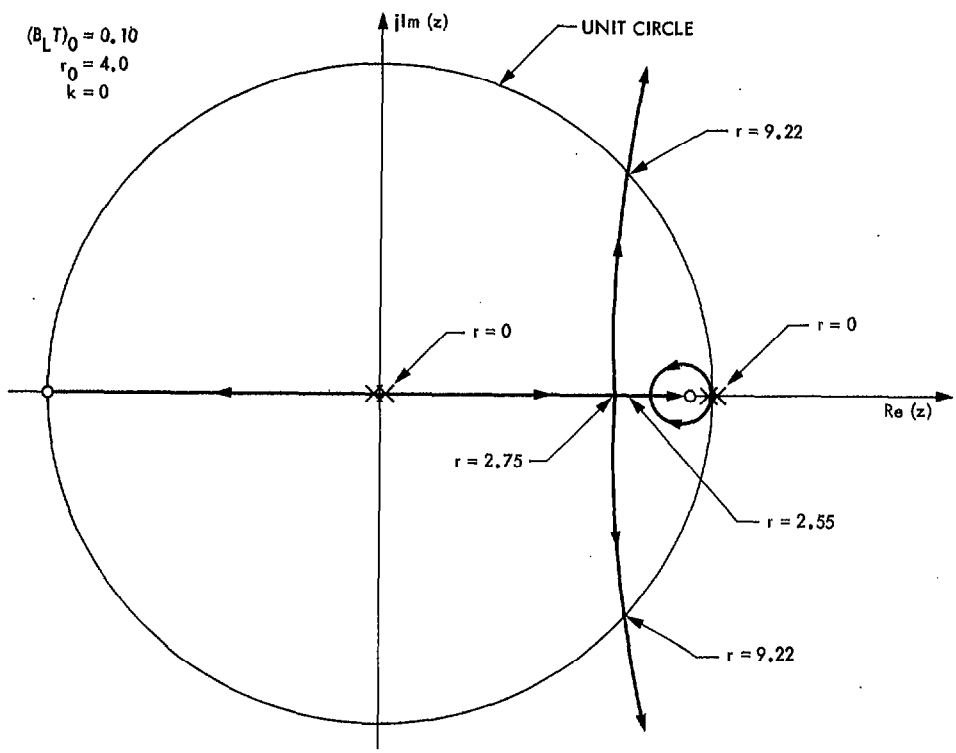

Fig. 4. Root locus of the second-order DPLL

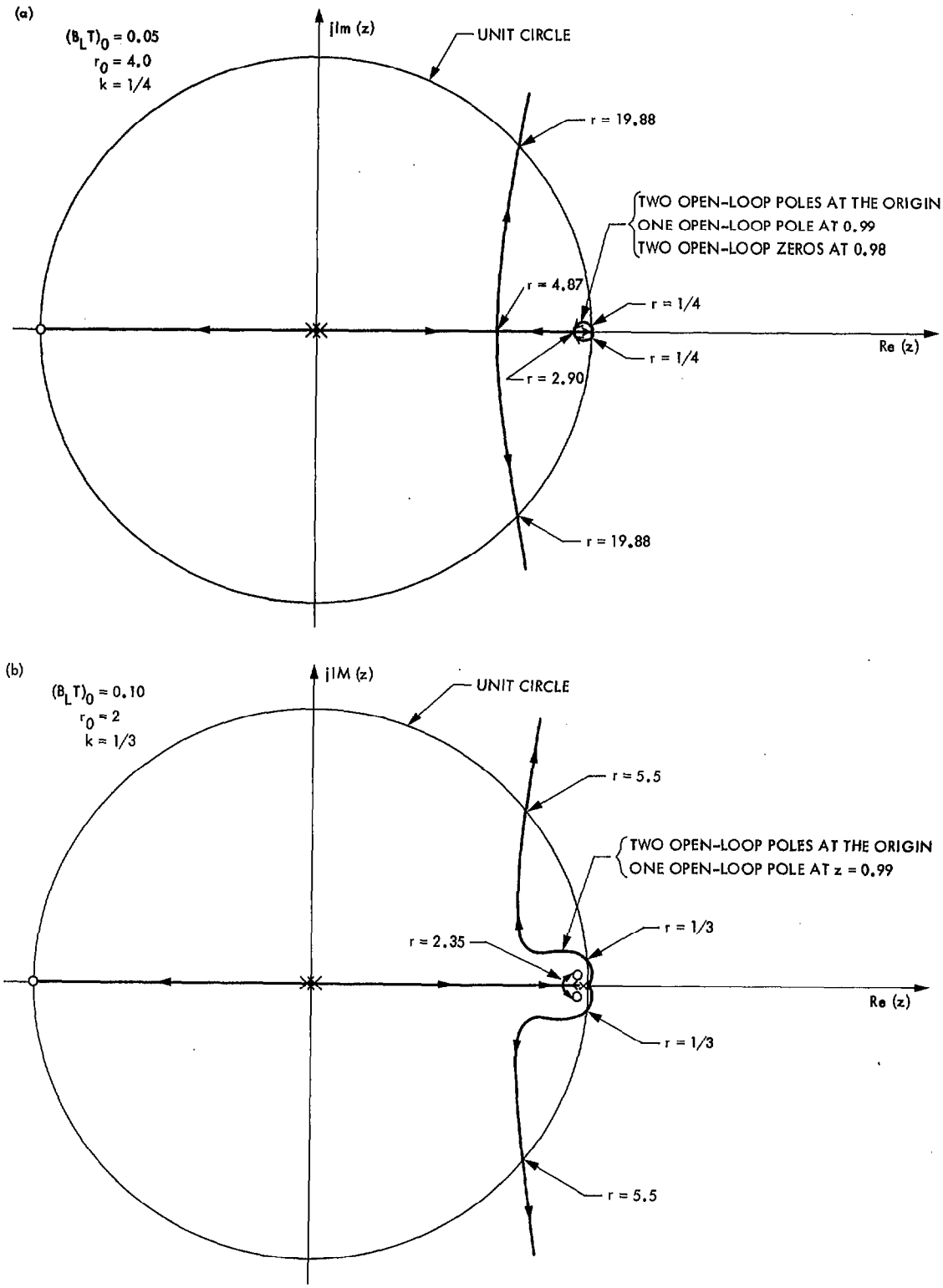

Fig. 5. Root loci of the third-order DPLL: (a) narrow bandwidth; (b) wide bandwidth, *underclamped*; (c) wide bandwidth with region of real roots

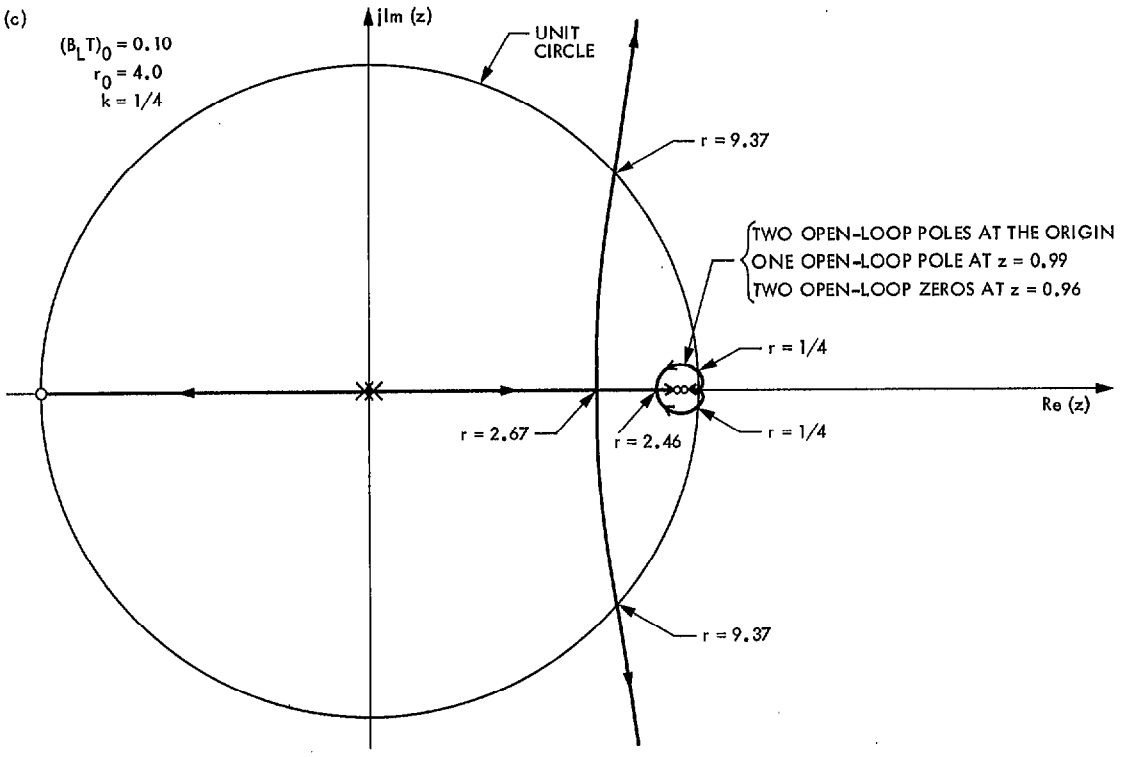

Fig. 5 (contd)

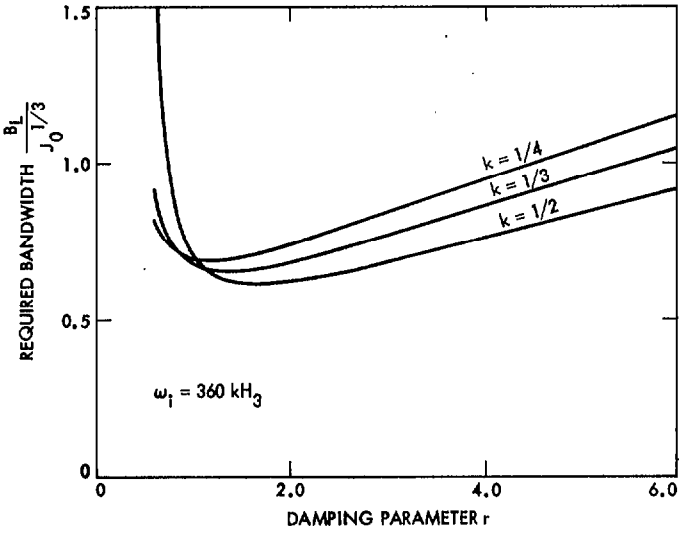

Fig. 6. Bandwidth requirements of third-order loops for 1° steady-state error

Appendix A
Derivation of N(z)

Figure A-1 is a block diagram of a DPLL with computation delay gT, i.e., for the case when the NCO input is updated gT seconds after the phase measurement is made. At the end of an integration interval of T seconds, the phase detector renders the difference of the average input phase and the average NCO phase.

Denote by $t_n = nT$ the sampling time, and by y_n the output of the NCO. We represent y_n with a linear piecewise function (see Fig. A-2) for g from 0 to 1,

$$y(t) = \begin{cases} y_{n-1+g} + x_{n-1} \cdot (t - t_{n-1+g}) & t_{n-1+g} \leqslant t \leqslant t_{n+g} \\ y_{n+g} + x_n \cdot (t - t_{n+g}) & t_{n+g} \leqslant t \leqslant t_{n+1+g} \end{cases} \tag{A-1}$$

the feedback function $\hat{\theta}_{n+1}$ is the averaged phase output over the interval from t_n to t_{n+1}, i.e.,

$$\hat{\theta}_{n+1} = \hat{\theta}_n + \frac{1}{T}\int_{t_n}^{t_{n+1}} y(\tau)\, d\tau \tag{A-2}$$

Performing the integration for intervals n and $n+1$, we obtain

$$\hat{\theta}_{n+1} = \hat{\theta}_n + \frac{1}{2}T[(1-g)^2 x_n + (1 + 2g - 2g^2) x_{n-1} + g^2 x_{n-2}] \tag{A-3}$$

Transforming to the z-domain, $N(z)$ is

$$N(z) \triangleq \frac{\hat{\theta}(z)}{x(z)} = \frac{T[(1-g)^2 z^2 + (1 + 2g - 2g^2)z + g^2]}{2z^2 (z - 1)} \tag{A-4}$$

For the advanced receiver implementation $g = 1$,

$$N(z) = \frac{T(z + 1)}{2z^2 (z - 1)} \tag{A-5}$$

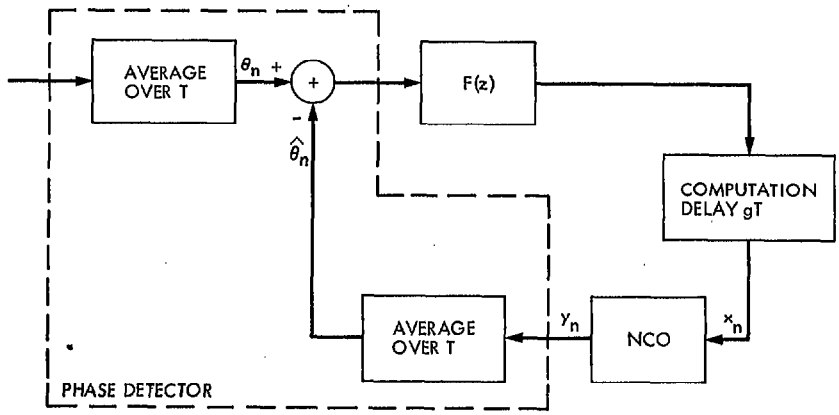

Fig. A-1. DPLL with computation delay *gT*

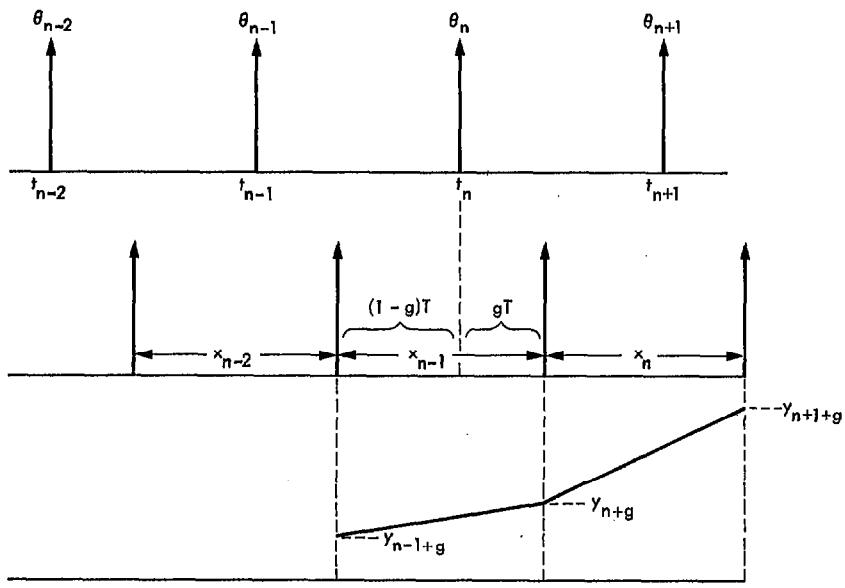

Fig. A-2. Timing for DPLL with computation delay *gT*